

# UC Irvine

## UC Irvine Previously Published Works

### Title

Revealing *Polylepis microphylla* as a suitable tree species for dendrochronology and quantitative wood anatomy in the Andean montane forests

### Permalink

<https://escholarship.org/uc/item/2q14c86w>

### Authors

Rodríguez-Morata, C.

Pacheco-Solana, A.

Ticse-Otarola, G.

et al.

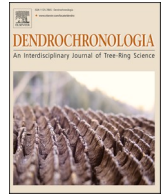
### Publication Date

2022-12-01

### DOI

10.1016/j.dendro.2022.125995

Peer reviewed



## Revealing *Polylepis microphylla* as a suitable tree species for dendrochronology and quantitative wood anatomy in the Andean montane forests

C. Rodríguez-Morata<sup>a,\*</sup>, A. Pacheco-Solana<sup>a</sup>, G. Ticse-Otarola<sup>b,i</sup>, T.E. Boza Espinoza<sup>c</sup>,  
D.B. Crispín-DelaCruz<sup>b,d</sup>, G.M. Santos<sup>e</sup>, M.S. Morales<sup>b,f</sup>, E.J. Requena-Rojas<sup>b,\*</sup>,  
L. Andreu-Hayles<sup>a,g,h,\*\*</sup>

<sup>a</sup> Lamont-Doherty Earth Observatory of Columbia University, Palisades, NY 10964, USA

<sup>b</sup> Laboratorio de Dendrocronología, Universidad Continental, Av. San Carlos 1980, Huancayo, Perú

<sup>c</sup> Institute for Nature, Earth and Energy (INTE), Pontificia Universidad Católica del Perú (PUCP), Av. Universitaria N° 1801, San Miguel, 15088 Lima, Perú

<sup>d</sup> Programa de Pós-Graduação em Ciências Florestais, Universidade Federal Rural de Pernambuco, Recife 52171-900, Brazil

<sup>e</sup> Department of Earth System Science, University of California, Irvine, B321 Croul Hall, Irvine, CA 92697-3100, USA

<sup>f</sup> Departamento de Dendrocronología e Historia Ambiental, Instituto Argentino de Nivología, Glaciología Ambientales (IANIGLA), C.C. 330, 5500 Mendoza, Argentina

<sup>g</sup> CREA, Bellaterra (Cerdanyola del Vallés), Barcelona, Spain

<sup>h</sup> ICREA, Pg. Lluís Companys 23, Barcelona, Spain

<sup>i</sup> Programa de Investigación de Ecología y Biodiversidad, Asociación ANDINUS, Calle Miguel Grau 370, Sicaya, Perú

### ARTICLE INFO

#### Keywords:

*Polylepis microphylla*

Andes

Dendrochronology

Quantitative wood anatomy

### ABSTRACT

In the tropical Andes climate change is expected to increase temperatures and change precipitation patterns. To overcome the lack of systematic weather records that limits the performance of climate models in this region, the use of the environmental information contained in tree rings from tropical Andean species have been found useful to reconstruct spatio-temporal climate variability. Because classical dendrochronology based on ring-width patterns is often challenging in the tropics, alternative approaches such as Quantitative Wood Anatomy (QWA) based on the measurement and quantification of anatomical traits within tree rings can be a significant advance in the field. Here we assess the dendrochronological potential of *Polylepis microphylla* and its climate sensitivity by using i) classic dendrochronological methods to generate the first Tree-ring Width (TRW) chronology for this tree species spanning from 1965 to 2018; ii) radiocarbon (<sup>14</sup>C) analyses as an independent validation method to assess the annual periodicity of the tree growth layers; and iii) QWA to generate tree-ring annual records of the number (VN) and size (VS) of vessels to investigate the climate sensitivity of these anatomical traits. The annual periodicity in *P. microphylla* radial growth was confirmed by both dendrochronological and <sup>14</sup>C analyses. We found that VN and VS are promising new proxies to reconstruct climate variability in this region and that they provide different information than TRW. While TRW provides information at inter-annual resolution (i.e., year-to-year variability), VN and VS generated with sectorial QWA provide intra-annual resolution for each stage of the growing process. The TRW and the anatomical traits (i.e., VN and VS) showed strong positive correlation with maximum temperature for different periods of the growing season: while VS is higher with warmer conditions prior to the growing season onset, tree-rings are wider and present higher number of vessels when warmer conditions occur during the current growing season. Our findings pointed out the suitability of *P. microphylla* for dendrochronological studies and may suggest a good performance of this species under the significant warming expected according to future projections for the tropical Andes.

\* Corresponding authors.

\*\* Corresponding author at: Lamont-Doherty Earth Observatory of Columbia University, Palisades, NY 10964, USA.

E-mail addresses: [clara.rodriguez@ldeo.columbia.edu](mailto:clara.rodriguez@ldeo.columbia.edu) (C. Rodríguez-Morata), [erequena@continental.edu.pe](mailto:erequena@continental.edu.pe) (E.J. Requena-Rojas), [lah@ldeo.columbia.edu](mailto:lah@ldeo.columbia.edu) (L. Andreu-Hayles).

<https://doi.org/10.1016/j.dendro.2022.125995>

Received 13 July 2022; Accepted 8 August 2022

Available online 28 August 2022

1125-7865/© 2023 The Authors. Published by Elsevier GmbH. This is an open access article under the CC BY-NC-ND license (<http://creativecommons.org/licenses/by-nc-nd/4.0/>).

## 1. Introduction

Weather and climate over the Andes is driven by the large-scale atmospheric circulation patterns over South America, which are influenced by the Andean topography (Espinosa et al., 2020). The Andes hosts a high biological diversity, agrobiodiversity, and endemism (Buytaert et al., 2011; de Haan, 2009), as well as water provision to mining, agricultural, energetic, and urban demands (Buytaert et al., 2011; Buytaert and de Bièvre, 2012; Vuille et al., 2008) conferring an important ecological relevance to this region. It is expected that climate change will decrease water provision in that region (Magrin et al., 2014) due to the reduction of annual precipitation driven by the shortening of the rainy season (Thibeault et al., 2010). Predictions also indicate that precipitation will be less frequent but more intense, increasing the risk of flood events and affecting the water regulation service (Thibeault et al., 2010) and thus, jeopardizing the functionality of ecosystems and services that they provide. On the other hand, projections of changes in the 21st century indicate significant warming in the tropical Andes, especially at high elevations (Urrutia and Vuille, 2009).

The understanding of climate variability and its drivers in the tropical Andes has been limited by the lack of a sufficient number of well spatially distributed ground-based meteorological stations recording precipitation and temperature (Condom et al., 2020), as well as by limitations from the Tropical Rainfall Measurement Mission (TRMM) Multi-satellite Precipitation Analysis (TMPA) due to biases of daily precipitation amounts and underestimation of rainfall events intensity (Scheel et al., 2011). This data scarcity hampers the assessment of trends, low-frequency variability and return time of extreme event occurrence such as severe droughts and floods. In this context, the development of new high-resolution precipitation and temperature proxies to extend this information back in time is crucial to assess the full range of climate variability in this region from inter-annual to decadal and centennial time scales.

The central Andean highlands, located between 10°S and 30°S, offer a great opportunity for dendrochronological studies due to a strong rainfall seasonality associated to the seasonal variability of the South American monsoon system (SAMS) (Carvalho and Cavalcanti, 2016), which occurs when the establishment of the Bolivian High brings easterly, moist-laden winds from the interior of the continent (Garreaud, 1999). The percentage of precipitation received during the rainfall season and its onset varies regionally in the Central Andes, with values ranging between 80% and 90% of the total annual amount for the Altiplano with a lower range (50–80%) in the Andean eastern slopes where the rainy season starts earlier (in October or November) and lasts until April (Vuille and Keimig, 2004). This marked seasonality in precipitation induces a dormancy period in plants (Josse et al., 2009) that translates in an annual formation of growth layers that register year-to-year variation in their wood properties such as ring-width, density, anatomical features and/or isotopic composition. Specifically, the Central Andes in Peru sustain one of the most diverse forests in the world (Josse et al., 2009). Several dendrochronological studies in the region, and further south in the Altiplano, found significant relationship between tree growth and environmental variables such as temperature and precipitation (Solíz et al., 2009; Ballantyne et al., 2011; Brien et al., 2012; Requena-Rojas et al., 2020, 2021; Crispin Dela Cruz et al., 2022; Rodríguez-Caton et al., 2021), as well as with El Niño Southern Oscillation (ENSO) variability (Christie et al., 2009; Li et al., 2013; Crispin Dela Cruz et al., 2022; Rodríguez-Caton et al., 2021), which explain much of the inter-annual hydroclimate variability in the Andes with reduced precipitation during ENSO warm phase and increase precipitation during ENSO cold phase (Garreaud et al., 2009).

Despite significant progress, tree-ring based climate reconstructions are still scarce in the tropical Andes (see the International Tree-Ring Data Bank; Grissino-Mayer and Fritts, 1997). Tree growth in the tropical Andes is influenced by multiple physical, biological, and climatic factors that lead to difficult interpretations of TRW patterns, challenging

the crossdating methods based on matching tree-growth patterns among distinct trees (Stahle, 1999; Groenendijk et al., 2014), and thus hampering the development of robust TRW chronologies in the Tropics. A promising alternative approach is the so called dendroanatomy, defined as the analysis of xylem-cell features within dated tree rings which can provide a long-term perspective on the wood formation process (Fonti et al., 2010). Quantitative Wood Anatomy (QWA) refers to the methodology that involves the generation of time series based on the measurement of anatomical traits within tree rings. Long histological sections allow for the characterization, quantification and analysis of wood anatomical traits of xylem throughout the plant's life and provide crucial insights into tree functioning and responses to past climate (e.g., Fonti and Jansen, 2012; Gärtner et al., 2014; von Arx et al., 2012). At the same time QWA allows for an intra-annual resolution not available when measuring the width of the rings (Wang et al., 2002). Up to date most QWA tree-ring chronologies have been mainly generated using boreal, Mediterranean and/or temperate tree species (e.g., Akhmetzyanov et al., 2019; Gärtner and Nievergelt, 2010; Gärtner et al., 2015a, 2015b; Ivanova et al., 2015), and to our knowledge only a few recent studies have explored QWA in tropical species in Brazil (Quintilhan et al., 2021; Ortega-Rodríguez et al., 2022).

One of the most important dendrochronological advances in South America has been the development of *Polylepis* spp. tree-ring chronologies. The genus *Polylepis* comprises small- to medium-sized evergreen angiosperm trees that cover large high-elevation areas about ~1800 to 5200 m a.s.l. (Simpson, 1979) along the Andes in South America from northern Venezuela to northern Chile and adjacent Argentina (8° N to 32° S) (Fig. 1a; Gosling et al., 2009; Zutta and Rundel, 2017; Cuyckens and Renison, 2018). *Polylepis tarapacana* has been the species most studied of the genus from a dendrochronological point of view (Argollo et al., 2004; Christie et al., 2009; Solíz et al., 2009; Morales et al., 2004, 2012, 2015; Moya and Lara, 2011) and it has been proven useful for reconstructing precipitation (Morales et al., 2012), ENSO variability (Christie et al., 2009; Li et al., 2013) and drought, expressed as the Palmer Drought Severity Index (PDSI), composing a tree-ring network that has been key for the generation of the South America Drought Atlases (Morales et al., 2020). The *P. tarapacana* network spans from 18°S to 23°S and was recently expanded north with a Peruvian chronology (17° 24' S - 69° 39' W; Crispin Dela Cruz et al., 2022). Other *Polylepis* species used in tree-ring research from north to south include *P. rodolfo-vasquezii* (11°43' S - 75°8' W; Requena-Rojas et al., 2020), *P. subsericans* (13°12' S - 72°05' W; Jomelli et al., 2012), *P. rugulosa* (15° 40' S - 75° 48' W; Jomelli et al., 2012), *P. pepeii* (17° 00' S - 65° 39' W; Roig et al., 2001), *P. besseri* (17° 44' S - 65° 34' W; Gareca et al., 2010) and *P. australis* (~32° S; Chartier et al., 2016; Marcora et al., 2017; Suarez et al., 2008). The success of this genus expanding the distribution of dendrochronological proxy records into the tropical region is related to the presence of well-defined annual rings and high climatic sensitivity, as well as the longevity and unique geographical locations where often no other tree species are present and/or show well-defined tree rings (Boninsegna et al., 2009). Remarkably, Peru hosts the highest number of species of the genus with a total of 23 *Polylepis* species (Boza, 2020), being many of them still uninvestigated from a dendrochronological point of view.

*Polylepis microphylla* has been reported to grow in several locations of Peru and Ecuador between 3200 and 4300 m a.s.l. (Fig. 1a). It was first described in 1861 as *P. lanuginosa* var. *microphylla* (Weddell, 1861), but the classification of this species has changed several times since then. In the year 1911 *P. microphylla* was classified as a tree species for the first time (Bitter, 1911), but in 1979 a further review reclassified it as a variety of *P. weberbaueri* (Simpson, 1979). Finally, *P. microphylla* was accepted as tree species in 1996 (Romoleroux, 1996).

The objectives of this paper are the assessment of the dendrochronological potential of *Polylepis microphylla* and its climate sensitivity. Specifically, we will use classic dendrochronology to generate the first TRW chronology for *P. microphylla* and will assess the annual periodicity

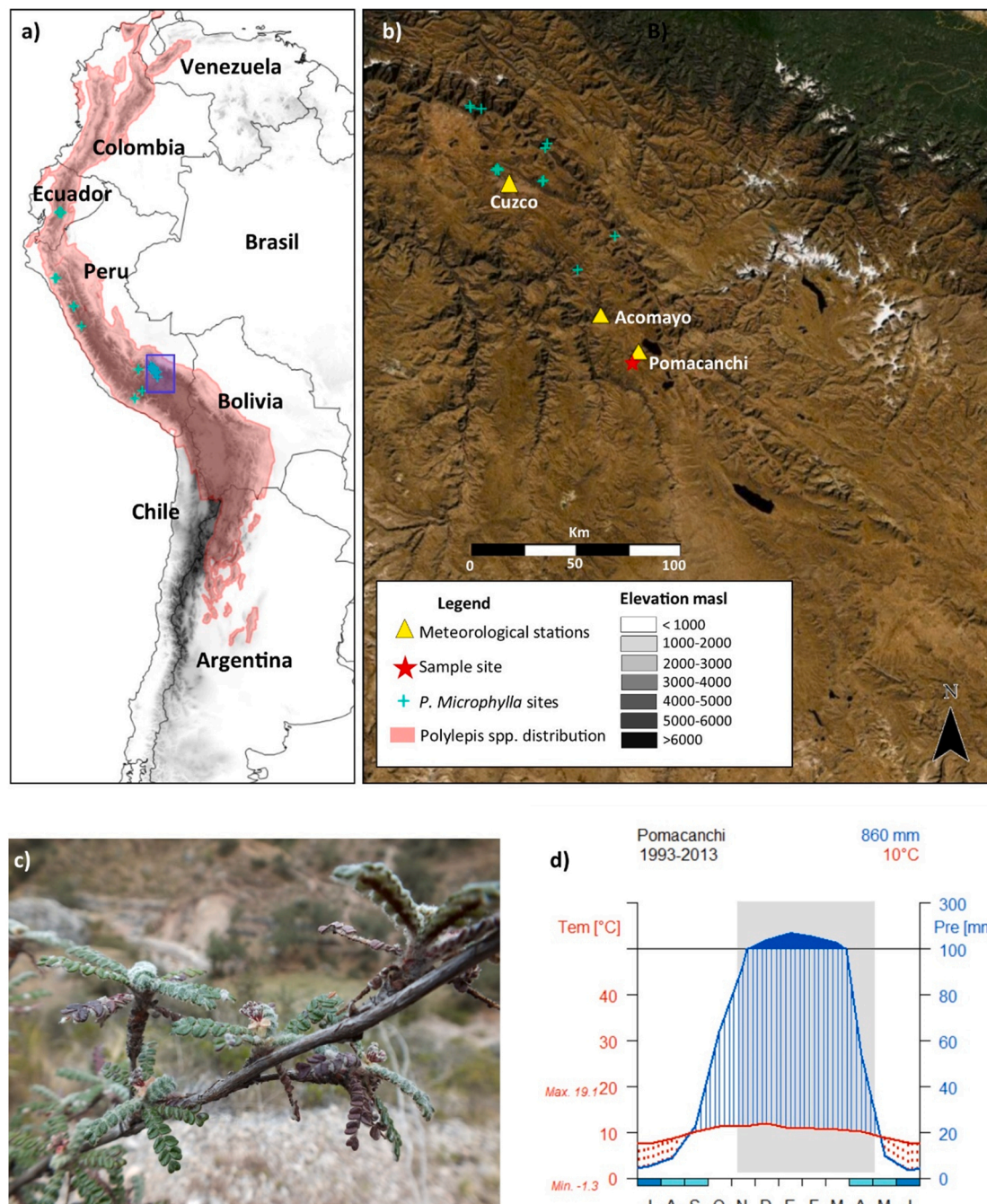


**Fig. 1.** a) Pink shaded area indicates the *Polylepis* spp. geographic distribution from 8°N to 32°S in an altitudinal range of ~1800 to 5200 m a.s.l. (Simpson, 1979; Boza and Kessler, 2022) *Polylepis microphylla* specimens (green crosses) has been identified in sites at Ecuador and Peru growing between 3200 and 4300 m a.s.l. (Boza 2020, Boza and Kessler, 2022). Blue square represents the study region. b) Map of the study region in the Peruvian Andes indicating the *P. microphylla* site in Pomacanchi (red star) and the three closest meteorological stations to our study site (yellow triangles). c) Picture of *P. microphylla* leaves and flowers. d) Walter-Lieth climatic diagram for the study site. Mean annual temperature is ~10 °C and mean total precipitation is 860 mm. Wet period (blue vertical lines) starts in late September to early May with a rainfall peak (solid blue area, monthly precipitation  $\geq 100$  mm) between November and March. The growing season, running from November to April according to Servat et al. (2013), is highlighted in gray.

of the tree growth layers using radiocarbon ( $^{14}\text{C}$ ) analyses as an independent validation method. Further, we will use a dendroanatomy approach over well-dated rings to generate tree-ring time series of the number and size of vessels to investigate if these anatomical traits can provide distinct seasonal climate information than radial growth (i.e., TRW).

## 2. Material and methods

### 2.1. Study site

This study was carried out at the Pomacanchi district in the Peruvian Central Andes (14° 4.02' S – 71° 35.15' W) at 4295 m a.s.l. in the Cuzco region (Fig. 1a, b). The study site belongs to the high altitude Puna phytogeographical region that encompasses a latitudinal range between

6°S to 23°S and an elevation above 3500 m a.s.l. in the Central Andes. This region is characterized by hosting diverse ecosystems of grasslands and open shrub lands. *Polylepis microphylla* grows as shrub or small multi-stem trees that may reach 1.5–8 m tall; leaves are compound imparipinnate with 3–6 pairs of lateral small leaflets and strongly congested at the branch tips (Fig. 1c); the inflorescences present from 1 to 3 small green flowers; the fruits have variable numbers of long spines. *Polylepis microphylla* have been found as isolated populations (Fig. 1a) located in the Ecuadorian Andes on the slopes of the Chimborazo volcano (Romoleroux, 1996) and in Peru at the northwestern region in the high Andes of Cajamarca, the Cordillera Blanca and the adjacent Cordillera of Huayhuash, at the boundaries of Ancash and Lima regions, and at the southern region in Arequipa and Cusco (Boza, 2020). It grows mainly in arid zones where it usually creates small groves with most of the patches formed by small young shrubs in areas strongly affected by human activities at 3150–4550 m a.s.l. (Boza, 2020; Boza and Kessler, 2022). At Pomacanchi, the mean annual temperature is ~10 °C and the annual total precipitation oscillates between 1070 and 603 mm based on the closer meteorological station (Pomacanchi station, 14° 2' S – 71° 34' W; 3690 m a.s.l.) with a rainfall season spanning from late September to early May, being the rainiest period from November to March (Fig. 1d).

## 2.2. Sample collection and preparation

Sample collection was done in July 2019 in a random scheme selecting the larger individuals along an altitudinal range between 3995 and 4017 m a.s.l. Using a manual hand saw we collected cross sections from one stem of 26 multi-stem living and dead trees. We discarded trees with evident physical damages associated to fires or another disturbance (i.e., cattle, windstorms, etc). For this study, we used samples from the nine older living trees, which also exhibited the clearest ring growth pattern. We acknowledge the low number of samples but due to the exploratory nature of this work we consider this number sufficient to test the objectives of this study. The remaining samples are being analyzed and they will be added to the master chronology in the near future. The samples were dried at air temperature and polished with increasingly finer sandpaper (from 80 to 1500 grit) to allow for a good visualization of ring boundaries and anatomical features under a stereomicroscopy (Orvis and Grissino-Mayer, 2002; Gärtner et al., 2015a).

## 2.3. Tree-ring Width chronology development

We first visually cross-dated tree rings under a stereomicroscope considering TRW patterns. Following the Southern Hemisphere convention annual rings were assigned to the calendar year in which their formation began (Schulman, 1956). In our case since the samples were collected in July 2019, the last complete ring next to the bark was assigned to 2018. We scanned the samples with a 3200 dpi resolution using an EPSON Expression 11000XL scanner and measured the width of the tree rings using Coorecorder 9.6 software. Then, we performed a statistical quality control of the crossdating to solve possible errors in relation to absent or false rings using the COFECHA software (Holmes, 1983).

To build the chronology the individually dated TRW time series were detrended and standardized using a cubic-smoothing spline with a 50% frequency response of 20 years to minimize short-period growth excursions associated with non-climatic (Fritts, 1976) dynamics using the 'dplr' package for R software (Bunn, 2008). The resulting individual TRW time series were averaged using the *chron* function of the same package. This function builds a mean value chronology that uses a robust mean to obtain the TRW chronology expressed as a Ring-width Index (RWI). To validate the strength of the TRW chronology, we calculated summary statistics, including the mean inter-series correlation ( $r$ ), Expressed Population Signal (EPS), and Subsample Signal Strength (SSS). The inter-series correlation is calculated by removing each core from the chronology to correlate it with a master chronology

generated with the rest of individual time series over the common interval. The EPS and SSS are both metrics of the strength of a common signal shared by the time series within the trees and between the trees. Usually, a value of  $\text{EPS} \geq 0.85$  is considered good for dendroclimatic reconstructions and a threshold value of  $\text{SSS} \geq 0.85$  determines the most reliable time span of the chronology (Wigley et al., 1984).

## 2.4. Radiocarbon analyses

We performed an independent validation of our dendrochronological dating using high-precision  $^{14}\text{C}$  bomb pulse dating of selected *Polylepis microphylla* tree rings. The  $^{14}\text{C}$  bomb pulse refers to the sudden increase of  $^{14}\text{C}$  in the Earth's atmosphere as a consequence of multiple above ground nuclear bombs tests occurring during the late 1950s and early 1960s and posterior decrease associated to the partial Nuclear Test Ban in 1963, which tagged all living organisms (Hua et al., 2021 and references therein). We chose four consecutive calendar years 1970, 1971, 1972 and 1973 (i.e., years when the tree growth started; Schulman, 1956) from the post-bomb period which were tested through  $^{14}\text{C}$  analysis of  $\alpha$ -cellulose extracts. Extraction of  $\alpha$ -cellulose was attained by a recently implemented procedure at the Lamont-Doherty Earth Observatory (LDEO; Andreu-Hayles et al., 2019) with the addition of one additional step of 1 N HCl 70 °C for 30 min to eliminate residues of acetic acid and  $\text{CO}_2$  that could be captured during the extraction process (Santos et al., 2020). The sample preparation for  $^{14}\text{C}$  analysis consisted first in a careful separation of each tree ring from the main wooden block using a scalpel. Tree rings were further chopped into wood slivers of about < 1 mm and the dry weight was measured. For *P. microphylla* a minimum of 5 mg of wood was requested to obtain about 1 mg of  $\alpha$ -cellulose after chemical proceedings with a minimum extraction yield of 19% (see Table 2 for all the values). Then the wood material was placed in individual funnels to undergo several chemical treatments. Background corrections and quality control determinations for high-precision  $^{14}\text{C}$  measurements were achieved through analysis of  $\alpha$ -cellulose extracts of reference materials, such as FIRI-J (post-bomb barley mash), FIRI-H (sub-fossil wood) and AVR (wood-blank). More details about the cellulose extraction proceeding can be found in Andreu-Hayles et al. (2019) and Santos et al. (2020), while further details about subsequent analytical procedures of  $^{14}\text{C}$  samples at Keck Carbon Cycle Accelerator Mass Spectrometer (KCCAMS) at the University of California, Irvine (UCI) are described in Santos and Xu (2017) and in Beverly et al. (2010).

## 2.5. Quantitative wood anatomy (QWA)

The cell anatomical measurements were performed on a sub-sample of five trees as its common practice in QWA (von Arx et al., 2016). The selected cross sections were cut into 4-cm long pieces, boiled in water in order to soften the wood and sliced into 10–12  $\mu\text{m}$  thick transversal sections using a core-microtome (Gärtner and Nievergelt, 2010). The samples were stained with safranin (1%) and astrablue (0.5%), both diluted in distilled water, and rinsed with water and ethanol. Afterwards they were fixed on permanent slides with Eukitt® Quick-hardening mounting medium (Sigma-Aldrich). Digital images were captured using an AmScope 12 MP Color CMOS Digital Eyepiece Microscope Camera installed in a light transmission microscope (Leitz, Laborlux 11, Type 020–435.028) using magnifications of 40X, 100X and 200X. The obtained images went through a semi-automatically analysis using the ROXAS v3 software (von Arx and Carrer, 2014). ROXAS provided measurements of cells regarding lumen area and cell-wall thickness while assigning to each measured cell its relative position within five equal segments along the dated annual ring (Fig. 2a).

We focused on vessel cells that correspond to cells bigger than 300  $\mu\text{m}^2$ . This threshold was a breakpoint of cell size distribution that efficiently separated the bigger vessel cells from the smaller fiber cells within each ring (Fig. 2b). Our approach was based on the assumption

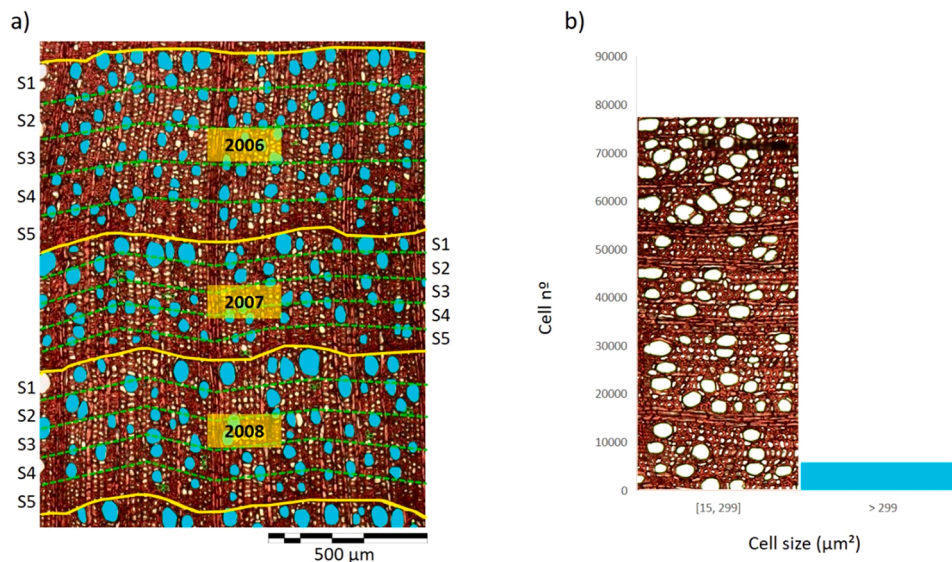


**Fig. 2.** a) ROXAS output sample showing the five sectors analyses. Vessels  $\geq 300 \mu\text{m}^2$  are highlighted in light blue and the ring boundaries in yellow. b) Histogram illustrating the average cells distribution by size and highlighting the breakpoint at  $300 \mu\text{m}^2$ .

that cells of larger diameter may have a more important functional role in relation to water transportation vertically along the tree stem and thus, yearly variations in their size and number can potentially be sensitive to climate variability. Since early and latewood are not visible in *Polylepis microphylla* each tree ring was divided into five sectors of equal relative width, named S1 to S5 (Fig. 2a), and each vessel was assigned to its corresponding sector. This division allows us to measure and analyze the number and size of vessels formed during successive periods over the growing season (Castagneri et al., 2017).

Time series of number of vessels (VN) and mean size of vessels (VS) were generated for each sector and every ring separately for the entire time span for each tree, and then the individual timeseries were averaged. The VN was calculated as a percentage for each single sector and ring at each sample (Eq. 1). Similarly, the mean individual VS was calculated by each ring (or sectors), as a regular average of the cells with areas bigger or equal to  $300 \mu\text{m}^2$ , divided by the total number of cells bigger or equal to  $300 \mu\text{m}^2$  (Eq. 2). For calculating the metric VS, was necessary normalizing (ZVS) each time series using the mean ( $\bar{X}VS$ ) and standard deviation ( $\sigma VS$ ) of each tree for the period 1968–2018 (Eq. 3) to account for relative TRW differences between rings and give equal importance to the five trees.

$$VN(\%) = (n^{\circ} \text{cells} \geq 300 \mu\text{m}^2 * 100) / \text{Total cells} \quad (1)$$

$$VS = \sum (\text{area cells} \geq 300 \mu\text{m}^2) / (\text{Total cells} \geq 300 \mu\text{m}^2) \quad (2)$$

$$ZVS = (VS - \bar{X}VS) / \sigma VS \quad (3)$$

## 2.6. Climate and tree growth relationship

There are three meteorological stations relatively close to the study site with available monthly records of precipitation, maximum temperature ( $T_{\text{max}}$ ) and minimum temperature ( $T_{\text{min}}$ ) (see station locations at the map in Fig. 1a and Table 1 for more details; data available at

**Table 1**  
Meteorological stations (see also Fig. 1b).

Name	Climate data	Data period	Latitude (S)	Longitude (W)	Elevation (m a.s.l.)	Distance to study site (Km)
Cuzco	P	1937–2016	13°31′	71°55′	3249	70
Acomayo	P, $T_{\text{max}}$ , $T_{\text{min}}$	1964–2013	13°55′	71°41′	3212	20
Pomacanchi	P, $T_{\text{max}}$ , $T_{\text{min}}$	1985–2013	14°2′	71°34′	3716	5

<http://www.senamhi.gob.pe/?p=download-hydrometeorological-data>). Data from these three datasets correlated well. We selected data from the Pomacanchi station because it may better represent the climate variability at our study site due to its closer proximity. From this station we used the last 20 years of climate data (1993–2013) without data gaps. Based on phenological studies from other *Polylepis* species (Servat et al., 2013) and on the onset of the wet season (Fig. 1d), we assumed that the growing season may span approximately from November to April at our study site.

To define the relationship between *Polylepis microphylla* growth and local climate, we computed Pearson's correlations between the tree-ring time series (i.e., TRW, VN and VS) and climate variables (i.e., precipitation,  $T_{\text{max}}$  and  $T_{\text{min}}$ ) using the “dcc” function from the Treecim R package (Zang and Biondi, 2015). The level of significance and confidence intervals of the correlation coefficient was assessed by bootstrap correlation analysis (Politis and Romano, 1994). Our analysis was done over two consecutive growing seasons spanning from August of the previous year to May of the current year to account for potential lagged effect of precipitation and temperature from previous year on the current tree growth (Fritts, 1971).

## 3. Results

### 3.1. The Tree-ring Width chronology and annual growth periodicity

*Polylepis microphylla* presented clearly distinguishable growth rings, delimited by a line of large vessels at the beginning of the earlywood and by the occurrence of thick-wall latewood fibers with elongated lumen area parallel to the boundary (Figs. 2a and 3a). Vessels were mostly solitary and with no presence of tyloses (i.e., vessel occlusion due to the overgrowth of the protoplast of adjacent living parenchyma) distributed in a semi-ring pattern of porosity. Rays were heterogeneous with cells showing uni-seriate and multi-seriate patterns up to four-cell wide. These features facilitated the visual identification of the individual rings

and the application of dendrochronological techniques.

The *Polylepis microphylla* TRW chronology spanned 54 years from 1965 to 2018 and is based on twelve radii from nine trees (Fig. 3c). Visual synchronization of TRW patterns and statistical crossdating validation showed that the nine individuals shared similar growth variations. The series had an inter-correlation of 0.563 and a mean sensitivity of 0.326. The EPS and SSS indicated a relatively high common signal among trees, particularly from 1974 to 2018 when the SSS values overpassed the 0.85 threshold (Fig. 3c).

The dendrochronological calendar dates agreed with the results obtained using the high-precision  $^{14}\text{C}$  bomb pulse dating of selected *Polylepis microphylla* tree rings (Table 2). This confirms the annual periodicity of this tree species. The *P. microphylla*  $\text{F}^{14}\text{C}$  values measured for the rings 1970, 1971, 1972 and 1973 (year  $t$  corresponding to year when growth starts according to Schulman convention) matched very well with the atmospheric  $\text{F}^{14}\text{C}$  values from the South Hemisphere (SH) curve Zone 1–2 rather than to values from SH Zone 3 curve (Fig. 3b). The tree-ring  $\text{F}^{14}\text{C}$  values agreed well to any of  $\text{F}^{14}\text{C}$  curve value of SH Zone 1–2 for the months corresponding to the growing season from November ( $t$ ) to April ( $t + 1$ ). For plotting purposes, our samples were visually matched to February  $\text{F}^{14}\text{C}$  SH curve value because this month approximately may represent the middle of the growing season. However, tree-ring  $\text{F}^{14}\text{C}$  values are also very close to the November–April average  $\text{F}^{14}\text{C}$  curve (Fig. 3b, Table 2). After chemical proceedings, cellulose extraction yield for *P. microphylla* ranged between 19.9% and 31.1% (Table 2). Radiocarbon results from reference materials, FIRI-J, FIRI-H and AVR, which undergo the LDEO  $\alpha$ -cellulose extraction, returned values within expected ranges (Santos et al., 2020).

### 3.2. Quantitative wood analysis

We analyzed a total of 25,790 vessels (cells  $\geq 300 \mu\text{m}^2$ ) from five

trees, with an average of 5158 vessels per tree (absolute maximum and minimum values of 6203 and 4401 vessels, respectively). Fig. 4 represents the VN and VS tree-ring records with the TRW chronology in the background. The correlation coefficients ( $R$ ) between the time series are indicated in the Table 3 and in Fig. 4 (top left).

The *Polylepis microphylla* VN, represented as percentage, exhibited a positive trend over time with a minimum vessel number of 2.58% in 1980 and a maximum vessel number of 8.13% in 2018 (Fig. 4a). The variability between trees represented by the error bars, remained pretty constant over the study period. The proportion of vessels by sector changed over time with more variability from 1968 to 1992 becoming more regular after 1992 until the end of the period (Fig. 4b). In general, the presence of vessels progressively decreased from S1 (Minimum 20.9%, maximum 30%) to S5 (minimum 4.28%, maximum 17.7%). Correlation coefficients between RWI and VN by sector (red values Fig. 4b) were the highest in S1 and S5 with negative and positive values, respectively.

The *Polylepis microphylla* VS values averaged for all trees ranged from  $357 \mu\text{m}^2$  in 1970– $1022 \mu\text{m}^2$  in 2016 (Fig. 4c) with absolute minimum and maximum values of  $300 \mu\text{m}^2$  and  $2599 \mu\text{m}^2$ , respectively. The VS showed a strong upward trend in time. The variability between trees changed with two periods of high variability between 1982 and 1987 and 2005–2018. On average the VS was higher in sector S1 and it decreased towards sector S5 (S1:  $690.85 \mu\text{m}^2$ ; S2:  $630.43 \mu\text{m}^2$ ; S3:  $590.78 \mu\text{m}^2$ ; S4:  $521.39 \mu\text{m}^2$ ; S5:  $431.87 \mu\text{m}^2$ ) keeping this proportion between sectors year to year (Fig. 4d). The VS anomalies by sector changed throughout time (Fig. 4e) with negative anomalies before 1995; a 7-year period (1995–2001) with low anomalies: positive in S4 and S5 and negative in S1–S3; and a final period of positive anomalies starting in 2002. However, the VS variability between sectors fluctuates between years with peaks of strong negative and positive anomalies in S5 (negative: 1970, 1974, 1976, 1980, 1981, 1983, 1991, 1992; positive:

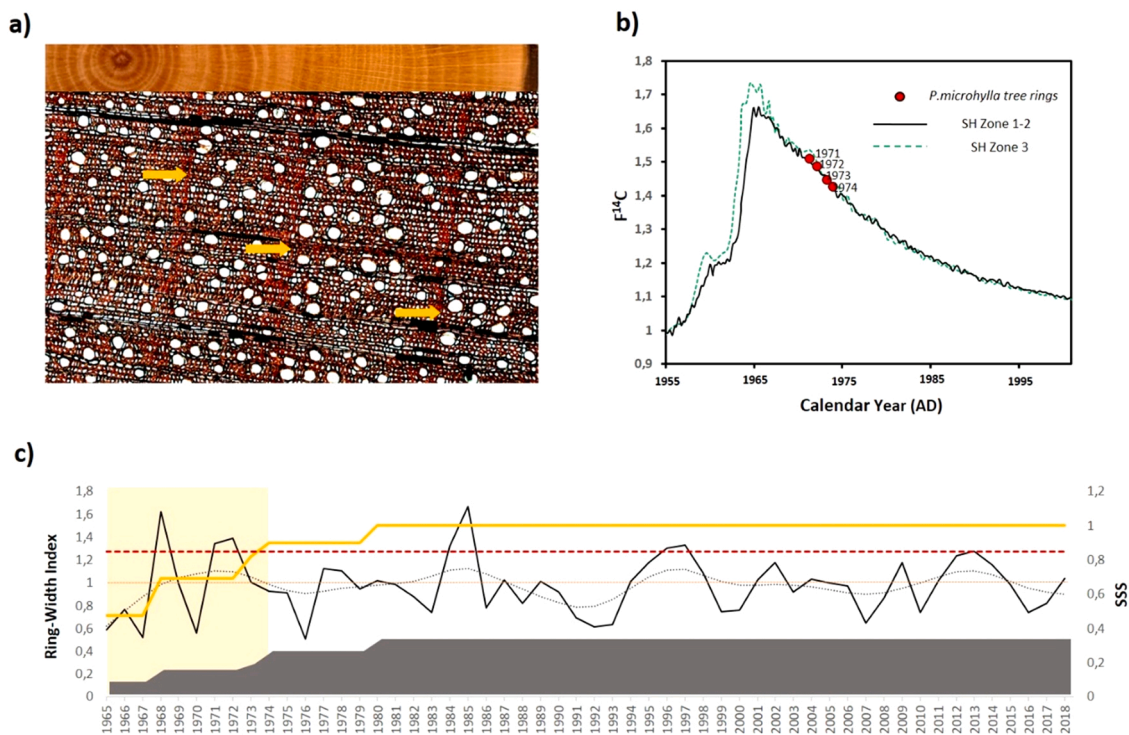


**Fig. 3.** a) Wood characteristics of *P. microphylla*. Growth rings are defined by the presence of big vessels at the beginning of the annual band and by fibers with thicker walls at the end (yellow arrows). b) Plot shows individual  $\text{F}^{14}\text{C}$  values of selected annual tree rings (red circles) from *P. microphylla* and the atmospheric  $\text{F}^{14}\text{C}$  values from SH Zone 1–2 and Zone 3 (Hua et al., 2021). For direct comparisons between selected annual tree rings and calendar dates derived from  $\text{F}^{14}\text{C}$  signatures, we added 1 year to Schulman's calendar year as well as a monthly adjustment of 0.125 that correspond to the month of February (see Table 2 for details). c) The *P. microphylla* TRW chronology (black line) is represented by the Ring-width Index with a 10-yr spline (grey dotted line). The SSS (yellow line), the 0.85 EPS critical value (dashed red line) and the total number of tree ring series, ranging from 2 to 12 series, included in the chronology (grey area) are shown.

**Table 2**

The  $^{14}\text{C}$  analysis for the *Polylepis microphylla* selected years. The dendrochronological calendar dates indicate the two calendar years when *P. microphylla* is growing, starting approximately in November- December (year  $t =$  Schulman year) and stopping around April (year  $t + 1$ ). A monthly adjustment based on the decimals values provided in the Supplementary material in Hua et al. (2021) was used. In our case, we used the decimals corresponding to February 15th (i.e., 0.1250) to plot the tree-ring  $\text{F}^{14}\text{C}$  over the SH  $^{14}\text{C}$  curves. The  $\text{F}^{14}\text{C}$  values from the SH  $^{14}\text{C}$  curves Zone 1–2 are indicated for February 15th and for the average from November to April that corresponds to the growing season (GS). The tree-ring  $\text{F}^{14}\text{C}$  values measured for this study are shown together with the uncertainty ( $\pm 1\sigma$ ) and UCIAMS#, which are the numeric codes for future reference at the UCI-KCCAMS facility. Finally, the amount of wood, cellulose material and the extraction yield are reported. All post-bomb  $^{14}\text{C}$  results are shown as  $\text{F}^{14}\text{C}$  signatures (Fraction Modern Carbon) as recommended in Reimer et al. (2004).

DENDROCHRONOLOGICAL CALENDAR DATES		RADIOCARBON INFORMATION					CELLULOSE EXTRACTION DETAILS			
T Year when tree start growing in austral spring -Schulman convention -	t + 1 Year when tree stop growing austral summer- fall.	*Monthly adjustment	$\text{F}^{14}\text{C}$ curve values (Hua et al., 2021) SH Zone 1–2		Radiocarbon tree-ring results and sample code.			Wood (mg)	Cellulose (mg)	Extraction yield (%)
			Feb (t + 1)	Average (GS) Nov (t) to Apr (t + 1)	$\text{F}^{14}\text{C}$	$\pm 1\sigma$	UCIAMS#			
1970	1971	1971.1250	1.5062	1.5073	1.5096	0.0021	256189	5.1	1.0	19.9
1971	1972	1971.1250	1.4803	1.4908	1.4872	0.0021	256190	10.1	3.0	30.0
1972	1973	1971.1250	1.4511	1.4582	1.4469	0.0019	256192	20.8	6.5	31.1
1973	1974	1971.1250	1.421	1.4208	1.4257	0.0019	256193	20.6	6.1	29.7

\* Decimals of the monthly adjustments correspond to February 15th as provided in Hua et al. (2021) Supplementary data.

(2018) and positive in S1-S3 (S1: 2007, 2008, 2010; S2 and S3: 2017) (Fig. 4e).

### 3.3. Relationship of TRW, VS and VN chronologies with climate

The Pearson correlation coefficients between the TRW chronology and climatic variables for the period 1993–2013 are shown in Fig. 5. TRW exhibited a positive relationship with  $T_{\text{max}}$  during most of the months of the current growing season, albeit they were only significant in October (R: 0.43) and in March (R: 0.53) (Fig. 5a). The correlation with the  $T_{\text{min}}$  was only significant with previous year January (R: -0.5), however there was a clear pattern of negative correlation coefficients prior to the current growing season becoming positive during the growing season (Fig. 5b). Regarding precipitation, there is a positive significant correlation between TRW and precipitation with current year September (R: 0.3) and November ( $r$ -value: 0.51) as well as with previous year September (R: 0.38) and December (R: 0.42) (Fig. 5c).

Figure 6 illustrates the correlation matrix summarizing relations between the TRW, VN and VS chronologies and the climatic variables (i.e., precipitation,  $T_{\text{max}}$  and  $T_{\text{min}}$ ). Regarding temperature (Fig. 6 a-f), the strongest correlation coefficient was found with  $T_{\text{max}}$  where VN and VS exhibited significant positive correlation with current year August (VN R= 0.5; VS R= 0.54), while TRW positively correlated with current year October (R= 0.44) and March (R= 0.52) (Fig. 6 a). At intra-annual scale, the VN (Fig. 6 b) in sectors S1 and S2 were significantly negative correlated with current year November (S1, R= -0.52) and October (S2, R= -0.4), while S3, S4 and S5 were positively correlated (i) with previous year August, September, October, November and April with significant correlation coefficients ranging between 0.7 (September in S4) to 0.44 (April in S3); (ii) in S4, with current year August (R= 0.43) and November (R= 0.4); and (iii) in S5, with current year October (R= 0.46), January (R= 0.5), March (R= 0.62) and April (R= 0.64). The VS in each sector (Fig. 6 c) consistently (positive) correlated across sectors and across months with  $T_{\text{max}}$ , with significant values particularly high for current year August ranging from 0.57 and 0.5 (S1 to S4) and for November with values of 0.5 (S1 and S2). From November onwards the  $T_{\text{max}}$  only correlated with VS in the sector S5 with current year January, March and April (R values between 0.3 to 0.36). Correlations with  $T_{\text{min}}$  exhibited a significant (negative) coefficient values regarding TRW with previous year January (R= -0.48) (Fig. 6 d) as well as with VN in some sectors (Fig. 6 e) with previous year August (S2, R= 0.52), February (S4, R= 0.56), April (S3, R= 0.56) and May (S4, R= 0.39) and with current year for the sector S5 in February (R= 0.55) and March (R= 0.5). The correlations between VS and  $T_{\text{min}}$  (Fig. 6 f) were not significant, however, there was a positive correlation pattern across all sectors with previous year November and December, as well as with the current

growing season from November to April. Regarding precipitation, correlation coefficients with TRW (Fig. 6g) indicated a significant positive values in previous year September (R= 0.38) and December (R= 0.42) and with current year September (R= 0.3) and November (R= 0.5). Significant correlation was also found for VS associated to previous year April (R= 0.32) and to current year August (R= -0.35) and October (R= -0.4) (Fig. 6g). The VN record did not show any significant correlation with precipitation. In contrast, considering the sectors, the strongest correlations were found for VN in S3 and S4 (Fig. 6 h) with significant values for previous year August to October (R values between -0.61 and -0.42). Significant positive correlations were only detected in S1 with previous year September (R= 0.5) and December (R= 0.53). The relationship between precipitation and VS (Fig. 6 i) was limited to current year August and October when all sectors exhibited negative significant correlation coefficients ranging from -0.39 to -0.33.

## 4. Discussion

Here we assessed the dendrochronological potential of *Polylepis microphylla*, a tree species never tested before from the Andean highlands of Peru and Ecuador. We developed the first TRW chronology of this species, as well as investigated its response to climate at seasonal and monthly scales. *Polylepis microphylla* exhibits clearly visible rings delimited by continuous rows of vessels at the beginning of the growing season contrasting with a narrow band of thick-wall fibers at the end of the ring which forms the latewood. These anatomic features are similar than those described to other species of the *Polylepis* genus such as *P. rodolfo-vasquezii* (Requena-Rojas et al., 2020), *P. tarapacana* (Argollo et al., 2004) and *P. pepeii* (Roig et al., 2001). The annual periodicity of *P. microphylla* growth was first supported by the successful cross-dating of the TRW patterns among the selected trees. The statistics used to verify the TRW chronology quality reported values of 0.563 for series inter-correlation, 0.326 for mean sensitivity and 0.738–0.85 for EPS, which indicated a relatively high common signal among trees, particularly in the chronology from 1974 to present (Fig. 3c). Other TRW chronologies from the Andes, previously documented similar values (Christie et al., 2009; Gareca et al., 2010; Jomelli et al., 2012; Morales et al., 2004; Moya and Lara, 2011; Roig et al., 2001; Solíz et al., 2009) pointing out *P. microphylla* as a promising Andean species to carry out dendrochronological studies. Furthermore, the results obtained with the measurement of high-precision  $^{14}\text{C}$  in four selected rings further confirmed the annual periodicity in *P. microphylla* growth.

We found that *Polylepis microphylla* radial growth represented by the TRW is actively modulated by the inter-annual variations of both, precipitation and temperature in this region (Figs. 5 and 6a, d, g). The results indicate that  $T_{\text{max}}$  is the primarily limiting factor controlling TRW



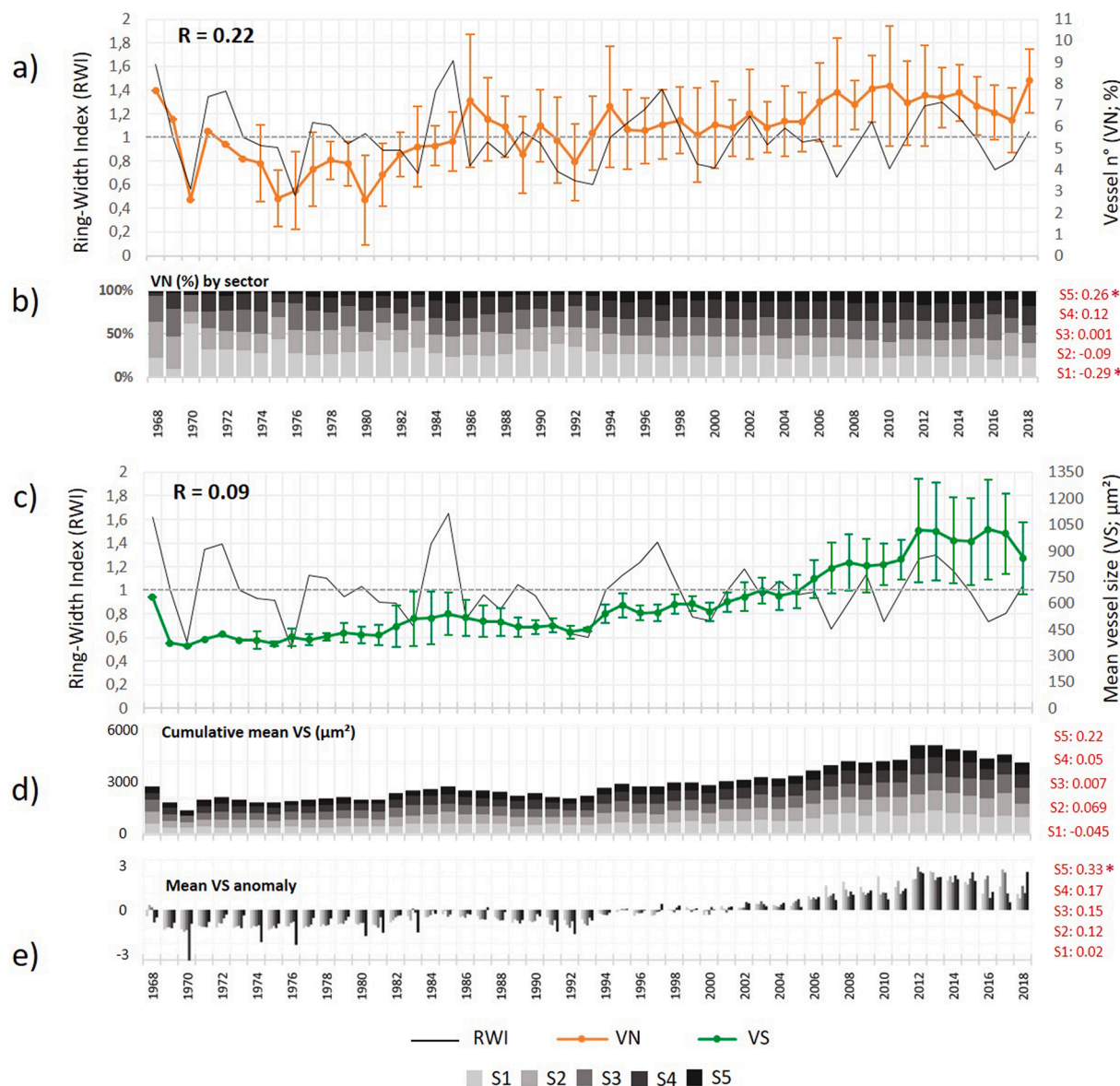


**Fig. 4.** a) VN time series (in orange) expressed by percentage ranging between 2.58% and 8.13%. b) VN by sector (in %) in relation to the total number of vessels for each ring. c) Mean VS time series (in green) ranging between 357  $\mu\text{m}^2$  in 1970–1022  $\mu\text{m}^2$  in 2016. d) Cumulative mean VS by sector throughout time. e) Mean VS anomalies by sector in relation to the average for each sector. The errors bars in a) and c) indicate the standard deviation of VN and VS for each year representing the variability among trees. Color bar in plots b), d) and e) indicate the five sectors from light grey (S1, early wood) to black (S5, late wood). The Ring-width Index (RWI) is shown by a black line in plot a) and b). The Pearson correlation values (R) between RWI and VN and VS records are indicated in the upper left corner for the entire ring (a, b) and in red for each sector (b, d, e). The correlation coefficient between VN and VS records is 0.75. Significant correlation coefficients ( $p < 0.05$ ) are indicated by asterisks.

**Table 3**

Pearson correlation coefficients between the TRW, vessel number and the vessel size records. Significant correlation coefficients ( $p < 0.05$ ) are indicated by black asterisks.

Correlation coefficients	Ring-width Index (RWI)	Vessel number (VN)	Vessel size (VS)
Tree-ring Width (TRW)	1	–	–
Vessel number (VN)	0.22	1	–
Vessels size (VS)	0.09	0.75*	1

during the current growing season (i.e., warm temperature may enhance growth) (Figs. 5a and 6a). These results are consistent with findings for other *Polylepis* species in Peru and the northern Bolivian Altiplano. For

example, Requena-Rojas et al. (2020) showed that *P. rodolfo-vasquezii* exhibited a solid positive relationship with current growing season temperature. Those chronologies were located in the Peruvian Andes farther north than our site (11°43' S – 75° 8' W), but at similar elevation (4360 to 4390 m a.s.l.) and equivalent total annual precipitation (~900 mm). South to our study site, populations of *P. tarapacana* growing at the southern border of Peru at 17°24' S – 69°39' W (4657 m a.s.l.; ~523 mm/ year precipitation) (Crispín-DelaCruz et al., 2022), as well as in Chile at 18°28' S – 69° 04' W (4600 m a.s.l.) and Bolivia at 19°06' S – 68° 27' W (4550 m a.s.l.) receiving ~300 mm of total annual precipitation (Rodríguez-Caton et al., 2021) also showed a strong temperature signal in the current year. In contrast, in southern *P. tarapacana* populations growing at 20°S and below (4400 – 4650 m a.s.l.) exposed to more arid conditions (~200 mm/year), tree growth was found to be more influenced by water availability with the TRW records positively

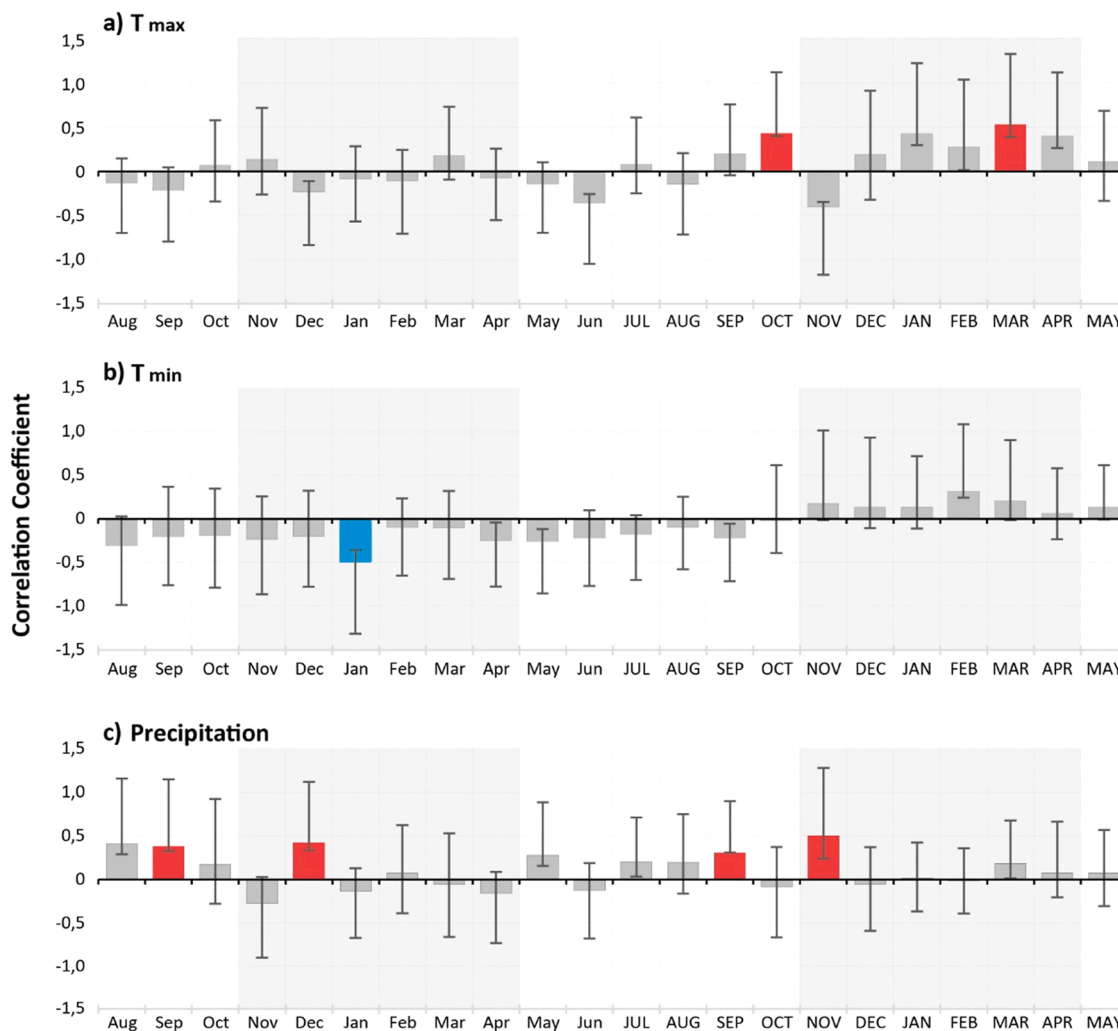


**Fig. 5.** Correlation coefficient between TRW and a)  $T_{max}$ , b)  $T_{min}$  and c) precipitation. The gray shaded areas represent the growing seasons from November to April. Significant correlation coefficients ( $\rho < 0.05$ ) are indicated by red (positive) and blue (negative) colored columns.

correlated with previous growing season precipitation (Argollo et al., 2004; Morales et al., 2004; Christie et al., 2009; Solíz et al., 2009; Rodríguez-Catón et al., 2021; Crispín-DelaCruz et al., 2022). In particular, the ecophysiology response of *Polylepis spp.* was found to vary being more sensitive to precipitation or temperature depending on the site location along a north-south aridity gradient with less water availability towards the south (Rodríguez-Catón et al., 2021). In other words, it seems that, when water requirements are met, the dominant factor controlling *Polylepis spp.* radial growth at high elevation in the Andes is temperature as commonly described in alpine treelines in extratropical forests (Oberhuber, 2007).

The *Polylepis microphylla* study site receives about 860 mm of annual precipitation (Fig. 1b), which is a considerably higher amount compared to other Andean locations further south. In addition, our site is located on a south-facing hillside receiving limited solar radiation, thus high levels of evapotranspiration and soil evaporation are not expected. Under this environmental condition water availability may not be a limiting factor for *P. microphylla*, thus radial growth can benefit from higher  $T_{max}$ , which may be also associated with more solar radiation, even though this implies less rainfall (i.e., less cloudiness). The association we found between TRW, previous growing season precipitation (Fig. 5 c) and current growing season  $T_{max}$  (Fig. 5 a) is consistent with results reported for *P. rodolfo-vasquezii* (Requena-Rojas et al., 2020) and *P. tarapacana* (Crispín-DelaCruz et al., 2022) that also pointed out that a wet spring-summer in the previous growing season together with warm

conditions during current season spring-summer is a favorable scenario for *Polylepis spp.* growing in sites without a limitation in water availability.

The newly generated QWA records of *Polylepis microphylla* vessel traits have been used to provide further insight on tree response to climate. The ROXAS software (von Arx and Carrer, 2014) quantifies in a very precise way the number, spatial distribution and size of the vessels. We observed a positive marked trend in the VN tree-ring record (Fig. 4a), which stabilized after 1992. Transversal and axial increases in conduit size have been proposed as the most efficient anatomical adjustment for stabilizing hydraulic path-length resistance during ontogeny of vascular plants, independent from species and plant size (Anfodillo et al., 2013; Carrer et al., 2015 and references therein). However, this increasing trend related to age-size growth is not the only signal retained in the conduit-dimension time series because certain environmental signatures can also be imprinted (Carrer et al., 2015). In this work we propose how to calculate two metrics, vessels size and vessel number, from all the anatomical trait data generated by the ROXAS software to generate annual and intra-annual vessel tree-ring records. Further investigations should focus on exploring additional metrics and detrending approaches to avoid potential biases and better retrieve environmental information from these new proxies.

The climate-vessel correlation analyses (Fig. 6) indicate that *Polylepis microphylla* vessels are more abundant (i.e., higher VN) with warmer conditions during the previous year spring-summer, especially for the

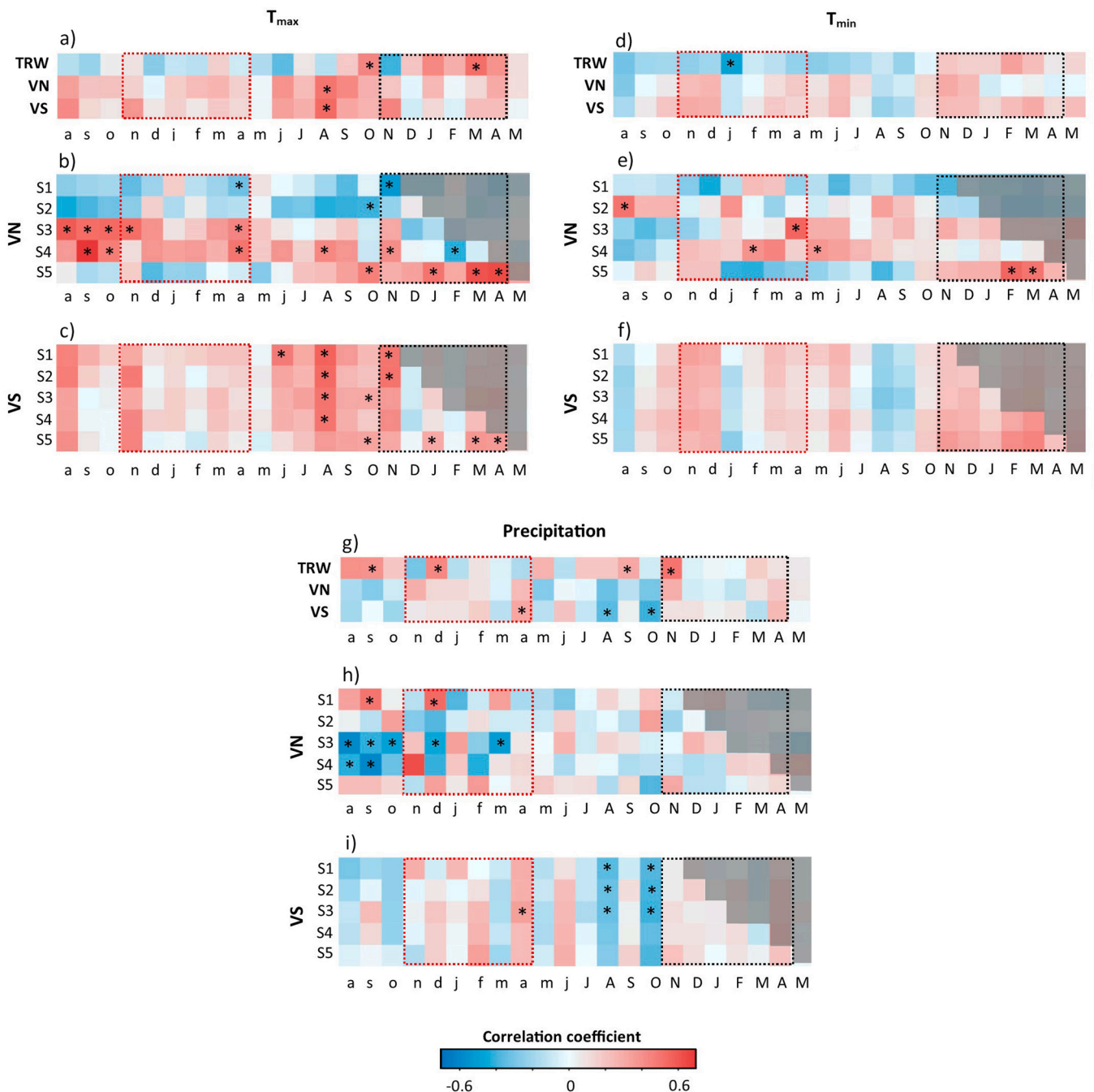


**Fig. 6.** Fig. 6 Correlation matrix illustrating associations between Tree-ring Width (TRW), vessel number (VN) and vessel size (VS) and the climatic variables (i.e., monthly precipitation,  $T_{max}$  and  $T_{min}$ ). Pearson correlations are shown from previous year August to current year May. Plots a, d) and g) show the correlation with TRW, VN and VS considering the average of the five sectors. Plots b, c, e, f, h and i represent the correlations using the VN and VS time series for the five sectors defined from the earlywood (S1) to the late latewood (S5). Significant correlation coefficients ( $p < 0.05$ ) are indicated by black asterisks. Grey shaded areas hide sectors no longer affected by climate throughout the growing season. Dotted squares represent current (black) and previous (red) growing seasons.

mid sectors of the ring (i.e., S3 and S4), while the last sector (i.e., S5) is correlated with the  $T_{max}$  during the current growing season (Fig. 6b). At the same time, the VN in sectors S1 and S2, exhibit negative correlations with  $T_{max}$  in October and November that may be linked to the slightly positive, not significant, correlation with precipitation in October, at the onset of growth (Fig. 6h). Similarly, the vessels are bigger (i.e., larger VS) with warmer (Fig. 6c) and drier (Fig. 6i) conditions prior to the growing season onset. In fact, this result contrasts with previous findings in other *Polylepis* species regarding VS and water-scarcity adaptation to avoid cavitation risk that reported a production of smaller but more abundant vessels related to low temperatures, low precipitation, and

high radiation levels (Camel et al., 2019). The negative correlation observed between precipitation and VS (i.e., bigger vessels when less precipitation) could be an artifact associated with temperature, which co-varies with precipitation, as reflected by the significant positive correlations found between VS and  $T_{max}$  during the previous dry season. In other words, it could be possible that *P. microphylla* VS did not benefit directly from less rainfall rather than high temperatures associated to clear skies (i.e., no rainfall).

*Polylepis microphylla* radial tree growth seems to be modulated by temperature thresholds controlling the start of cambial activity and modulating xylem cell differentiation during the growing season. This

temperature control over cambial activity has not been specifically tested in *Polylepis spp.*, however has been reported in alpine treelines in extratropical regions of the world. For example, in a study comparing species growth from cold climates in Europe and Canada, Rossi et al. (2008) found that wood formation in conifers occurred when specific minimum daily temperatures were reached during the growing season. Values below this threshold, while still favorable for photosynthesis, could inhibit the allocation of assimilated carbon to xylem growth. Another point of view in line with other studies in the Amazonian cloud forests is that higher temperatures during the current growing season are actually reflecting higher solar radiation (less cloud cover) which has been proved to enhance photosynthesis (Letts and Mulligan, 2005). During photosynthesis trees produce and assimilate carbohydrates, with some of these being used to build cellulose, favoring xylem production. The coupling of these two processes (i.e. photosynthesis and xylem formation) could be also related to being similarly favored by warmer conditions during the growing season in northern *P. tarapacana* sites (Rodríguez-Caton et al., 2021). However, same authors pointed out that both processes may decouple further south where xylem formation seemed to be limited by prior-climate conditions (Rodríguez-Caton et al., 2021).

## 5. Conclusions

Our study reports that *Polylepis microphylla* shows annually resolved well-defined tree rings which are suitable for dendrochronological studies. Here we developed the first *P. microphylla* TRW chronology, confirming this specie as a strong candidate to develop centennial chronologies if older individuals are found. In addition, the fact that this specie is sensitive to climate variability provides a new opportunity to fill gaps in a region with a noticeable lack of long-term instrumental records and tree-ring chronologies.

The incorporation of wood anatomy has proven to be a valuable addition to the classic dendrochronological approach, which is solely based in measuring the width of the tree rings. QWA is providing unique information at intra-annual scale on climate sensitivity and different tree hydraulic strategies depending on environmental conditions. Our results suggest that physiological processes determining VN and VS are mostly positively linked to  $T_{max}$  a few months before and during the growing season, as have been reported for in other *Polylepis* species. At the same time, precipitation occurring at the onset of the current growing season seems to positively influence the number of vessels generated during the first growth phases. Our findings suggest that *P. microphylla* could be an Andean tree species that may have good chances to adapt well to the warming expected for the 21st century for the central tropical Andes (Pabón-Caicedo et al., 2020). However, this adaptation would depend on future water availability for this region and climate projections show a large spread of precipitation among models, associated to as well as important uncertainties (Vera et al., 2006; Urrutia and Vuille, 2009).

## Declaration of Competing Interest

The authors declare that they have no known competing financial interests or personal relationships that could have appeared to influence the work reported in this paper.

## Acknowledgements

This work was supported by the U.S. National Science Foundation (NSF) projects AGS-1702789, OISE-1743738 and AGS-1903687; the U. S. National Science Foundation (NSF) projects AGS-1703035 and AGS-1903690; the *Fundação de Amparo à Ciência e Tecnologia do Estado de Pernambuco*—FACEPE (Process IBPG-1418–5.00/21); the *Agencia Nacional de Promoción Científica y Tecnológica*, Argentina (PICT 2013–1880); the *Consejo Nacional de Investigaciones Científicas y*

*Tecnológicas* (PIP 11220130100584); the THEMES project funded by the BNP Paribas Foundation in the frame of its 'Climate Initiative' program.

## References

- Akhmetzyanov, L., Buras, A., Sass-Klaassen, U., Ouden, J., Mohren, F., Groenendijk, P., García-González, I., 2019. Multi-variable approach pinpoints origin of oak wood with higher precision. *J. Biogeogr.* 46, 1163–1177. <https://doi.org/10.1111/jbi.13576>.
- Andreu-Hayles, L., Levesque, M., Martin-Benito, D., Huang, W., Harris, R., Oelkers, R., Leland, C., Martin-Fernandez, J., Anchukaitis, K.J., Helle, G., 2019. A high yield cellulose extraction system for small whole wood samples and dual measurement of carbon and oxygen stable isotopes. *Chem. Geol.* 504, 53–65. <https://doi.org/10.1016/j.chemgeo.2018.09.007>.
- Anfodillo, T., Petit, G., Crivellaro, A., 2013. Axial conduit widening in woody species: a still neglected anatomical pattern. *IAWA J.* 34, 352–364.
- Argollo, J., Soliz, C., Villalba, R., 2004. Potencialidad dendrocronológica de *Polylepis tarapacana* en los Andes Centrales de Bolivia. *Ecol. En. Bol.* 39, 5–24.
- von Arx, G., Carrer, M., 2014. ROXAS – a new tool to build centuries-long tracheid-lumen chronologies in conifers. *Dendrochronologia* 32, 290–293. <https://doi.org/10.1016/j.dendro.2013.12.001>.
- von Arx, G., Archer, S.R., Hughes, M.K., 2012. Long-term functional plasticity in plant hydraulic architecture in response to supplemental moisture. *Ann. Bot.* 109, 1091–1100. <https://doi.org/10.1093/aob/mcs030>.
- von Arx, G., Crivellaro, A., Prendin, A.L., Cufar, K., Carrer, M., 2016. Quantitative wood anatomy—practical guidelines. *Front. Plant Sci.*
- Ballantyne, A.P., Baker, P.A., Chambers, J.Q., Villalba, R., Argollo, J., 2011. Regional differences in South American monsoon precipitation inferred from the growth and isotopic composition of tropical trees. *Earth Interact.* 15 (5), 1–35.
- Beverly, R.K., Beaumont, W., Tautz, D., Ormsby, K.M., Santos, G.M., Southon, J.R., 2010. The keck carbon cycle AMS laboratory. *Radiocarbon* 52 (2), 301–309.
- Bitter, G., 1911. Revision der Gattung *Polylepis*. *Bot. Jahrb. Syst.* 45, 564–656.
- Boninsegna, J.A., Argollo, J., Aravena, J.C., Barichivich, J., Christie, D.A., Ferrero, M.E., Lara, A., C, L.Q., Luckman, B.H., Masiokas, M., Morales, M.S., J.M. O., Roig, F.A., Srur, A.M., Villalba, R., 2009. Dendroclimatic reconstructions in South America: a review. *Paleogeography, Paleoclimatol. Palaeoecol.* 281, 210–228. <https://doi.org/10.1016/j.paleo.2009.07.020>.
- Boza Espinoza, T.E., 2020. Taxonomies Studies in *Polylepis* (Rosaceae). Dissertation, University of Zurich, Switzerland.
- Boza Espinoza, T.E., Kessler, M., 2022. in press) A Monograph of the genus *Polylepis* (Rosaceae). *Phytokeys*.
- Brienen, R.J.W., Helle, G., Pons, T.L., Guyot, J.-L., Gloor, M., 2012. Oxygen isotopes in tree rings are a good proxy for Amazon precipitation and El Niño-Southern Oscillation variability. *Proc. Natl. Acad. Sci.* 109 (42), 16957–16962.
- Bunn, A.G., 2008. A dendrochronology program library in r (dplR). *Dendrochronologia* 26 (2), 115–124.
- Buytaert, W., de Bièvre, B., 2012. Water for cities: the impact of climate change and demographic growth in the tropical Andes. *Water Resour. Res.* 48, W08503.
- Buytaert, W., Cuesta-Camacho, F., Tobón, C., 2011. Potential impacts of climate change on the environmental services of humid tropical alpine regions. *Glob. Eco. Biogeogr.* 20, 19–33.
- Camel, V., Arizapana-Almonacid, M., Pyles, M., et al., 2019. Using dendrochronology to trace the impact of the hemiparasite *Tristerix chodatianus* on Andean *Polylepis* trees. *Plant Ecol.* 220 (2019), 873–886. <https://doi.org/10.1007/s11258-019-00961-w>.
- Carrer, M., von Arx, G., Castagneri, D., Petit, G., 2015. Distilling allometric and environmental information from time series of conduit size: the standardization issue and its relationship to tree hydraulic architecture. *Tree Physiol.* 35, 27–33.
- Carvalho, L., Cavalcanti, I., 2016. The South American monsoon system (SAMS). In: Carvalho, L., Jones, C. (Eds.), *The Monsoons and Climate Change*. Springer, Switzerland, pp. 121–148.
- Castagneri, D., Fonti, P., Von Arx, G., Carrer, M., 2017. How does climate influence xylem morphogenesis over the growing season? Insights from long-term intra-ring anatomy in *Picea abies*. *Ann. Bot.* 119, 1011–1020.
- Chartier, P.M., Alejandra, M., Renison, D., Roig, F.A., 2016. Exposed roots as indicators of geomorphic processes: a case-study from *Polylepis* mountain woodlands of Central Argentina. *Dendrochronologia* 37, 57–63. <https://doi.org/10.1016/j.dendro.2015.11.003>.
- Christie, D.A., Lara, A., Barichivich, J., Villalba, R., Morales, M.S., Cuq, E., 2009. El Niño-Southern Oscillation signal in the world's highest-elevation tree-ring chronologies from the Altiplano, Central Andes. *Palaeogeogr. Palaeoclimatol. Palaeoecol.* 281, 309–319. <https://doi.org/10.1016/j.paleo.2007.11.013>.
- Condom, T., Martínez, R., Pabón, J.D., Costa, F., Pineda, L., Nieto, J.J., López, F., Villacis, M., 2020. Climatological and hydrological observations for the South American Andes: in-situ stations, satellite and reanalysis data sets. *Front. Earth Sci.* 8, 92. <https://doi.org/10.3389/feart.2020.00092>.
- Crispín-DelaCruz, D.B., Morales, M.S., Andreu-Hayles, L., Christie, D.A., Guerra, A., Requena-Rojas, E.J., 2022. High ENSO sensitivity in tree rings. *Dendrochronologia* 71, 125902.
- Cuyckens, G.A.E., Renison, D., 2018. Ecología y conservación de los bosques montanos de *Polylepis*: Una introducción al número especial. *Ecol. Austral* 28, 157–162.
- Espinoza, J.C., et al., 2020. Hydroclimate of the Andes Part I: main climatic features. *Front. Earth Sci.* 8 (64).
- Fonti, P., Jansen, S., 2012. Xylem plasticity in response to climate. *New Phytol.* 195, 734–736. <https://doi.org/10.1111/j.1469-8137.2012.04252.x>.

- Fonti, P., Von Arx, G., García-González, I., Eilmann, B., Sass-Klaassen, U., Gärtner, H., Eckstein, D., 2010. Studying global change through investigation of the plastic responses of xylem anatomy in tree rings. *New Phytol.* 185, 42–53. <https://doi.org/10.1111/j.1469-8137.2009.03030.x>.
- Fritts, H.C., 1971. Dendroclimatology and dendroecology. *Quat. Res.* 1, 419–449. [https://doi.org/10.1016/0033-5894\(71\)90057-3](https://doi.org/10.1016/0033-5894(71)90057-3).
- García, E., Fernández, M., Atanot, S., 2010. Dendrochronological investigation of the high Andean tree species *Polylepis besseri* and implications for management and conservation. *Biodiversiti Conserv.* 19, 1839–1851. <https://doi.org/10.1007/s10531-010-9807-z>.
- Garreaud, R.D., 1999. Multiscale analysis of the summertime precipitation over the central Andes. *Mon. Weather Rev.* 127, 901–921.
- Garreaud, R.D., Vuille, M., Compagnucci, R., Marengo, J., 2009. Present-day South American climate. *Palaeogeogr. Palaeoclimatol. Palaeoecol.* 281, 180–195.
- Gärtner, H., Nievergelt, D., 2010. The core-microtome: a new tool for surface preparation on cores and time series analysis of varying cell parameters. *Dendrochronologia* 28, 85–92. <https://doi.org/10.1016/j.dendro.2009.09.002>.
- Gärtner, H., Lucchinetti, S., Schweingruber, F.H., 2014. New perspectives for wood anatomical analysis in dendro sciences: the GSL1-microtome. *Dendrochronologia* 32, 47–51. <https://doi.org/10.1016/J.DENDRO.2013.07.002>.
- Gärtner, H., Lucchinetti, S., Schweingruber, F.H., 2015a. A new sledge microtome to combine wood anatomy and tree-ring ecology. *IAWA J.* 36, 452–459. <https://doi.org/10.1163/22941932-20150114>.
- Gärtner, H., Cherubini, P., Fonti, P., von Arx, G., Schneider, L., Nievergelt, D., Verstege, A., Bast, A., Schweingruber, F.H., Büntgen, U., 2015b. A technical perspective in modern tree-ring research - how to overcome dendroecological and wood anatomical challenges. *J. Vis. Exp.* 1–10. <https://doi.org/10.3791/52337>.
- Gosling, W.D., Hanselman, J.A., Knox, C., et al., 2009. Long-term drivers of change in *Polylepis* woodland distribution in the Central Andes. *J. Veg. Sci.* 20, 1041–1052.
- Grissino-Mayer, H.D., Fritts, H.C., 1997. The international tree-ring data bank: an enhanced global database serving the global scientific community. *Holocene* 7 (2), 235–238.
- Groenendijk, P., Sass-Klaassen, U., Bongers, F., Zuidema, P.A., 2014. Potential of tree-ring analysis in a wet tropical forest: a case study on 22 commercial tree species in Central Africa. *Ecol. Manag.* 323, 65–78.
- de Haan, S., 2009. Potato Diversity at Height: Multiple Dimensions of Farmer-driven In-situ Conservation in the Andes. Wageningen University, The Netherlands.
- Holmes, R.L., 1983. Computer-assisted quality control in tree-ring dating and measurement. *Tree-Ring Bull.* 43, 69–78.
- Hua, Q., Turnbull, J.C., Santos, G.M., Rakowski, A.Z., Ancapichún, S., De Pol-Holz, R., Hammer, S., Lehman, S.J., Levin, I., Miller, J.B., Palmer, J.G., 2021. Atmospheric radiocarbon for the period 1950–2019. *Radiocarbon* 1–23.
- Ivanova, A., Dolezal, J., Gärtner, H., Schweingruber, F., 2015. Forty centimeter long transverse and radial sections cut from fresh increment cores. *IAWA J.* 36, 460–463. <https://doi.org/10.1163/22941932-20150115>.
- Jomelli, V., Pavlova, I., Guin, O., Soliz-Gamboá, C., Contreras, A., Toivonen, J.M., Zetterberg, J., 2012. Analysis of the dendroclimatic potential of *Polylepis pepel*, *P. subsericans* and *P. rugulosa* in the tropical Andes (Peru-Bolivia). *Tree-Ring Res.* 68, 91–103.
- Josse, C., Cuesta, F., Navarro, G., Barrena, V., Cabrera, E., Chácon-Moreno, E., Ferreira, W., Peralvo, M., Saito, J., Tovar, M., 2009. Ecosistemas de los Andes del Norte y Centro. Lima.
- Letts, M.G., Mulligan, M., 2005. The impact of light quality and leaf wetness on photosynthesis in north-west Andean tropical montane cloud forest. *J. Trop. Ecol.* 21, 549–557.
- Li, J., Xie, S.P., Cook, E., et al., 2013. El Niño modulations over the past seven centuries. *Nat. Clim. Change* 3 (2013), 822–826. <https://doi.org/10.1038/nclimate1936>.
- Magrin, G.O., Marengo, J.A., Boulanger, J.-P., Buckeridge, M.S., Castellanos, E., Poveda, G., Scarano, F.R., Vicuña, S., 2014. Central and South America. In: Barros, V. R., Field, C.B., Dokken, D.J., Mastrandrea, M.D., Mach, K.J., Bilir, T.E., Chatterjee, M., Ebi, K.L., Estrada, Y.O., Genova, R.C., Girma, B., Kissel, E.S., Levy, A. N., MacCracken, S., Mastrandrea, P.R., White, L.L. (Eds.), *Climate Change 2014: Impacts, Adaptation, and Vulnerability. Part B: Regional Aspects. Contribution of Working Group II to the Fifth Assessment Report of the Intergovernmental Panel on Climate Change*. Cambridge University Press, Cambridge, United Kingdom and New York, NY, USA, pp. 1499–1566.
- Marcora, P., Hensen, I., Renison, D., Seltmann, P., Wesche, K., 2017. The performance of *Polylepis australis* trees along their entire altitudinal range: implications of climate change for their conservation. *Divers. Distrib.* 14, 630–636. <https://doi.org/10.1111/J.1472-4642.2007.00455.X>.
- Morales, M.S., Villalba, R., Grau, H.R., Paolini, L., 2004. Rainfall-controlled tree growth in high-elevation subtropical treelines. *Ecology* 85, 3080–3089.
- Morales, M.S., Christie, D.A., Villalba, R., Argollo, J., Pacajes, J., Silva, S., Álvarez, C., Llanabure, J., 2012. Climate of the Past Precipitation changes in the South American Altiplano since 1300 AD reconstructed by tree-rings of the South Precipitation changes in the South American Altiplano since 1300 AD reconstructed by tree-rings. *Clim. Discuss.* 8, 653–666. <https://doi.org/10.5194/cp-8-653-2012>.
- Morales, M.S., Carilla, J., Grau, H.R., Villalba, R., 2015. Multi-century lake area changes in the Southern Altiplano: a tree-ring-based reconstruction. *Clim. Discuss.* 11, 1139–1152. <https://doi.org/10.5194/cp-11-1139-2015>.
- Morales, M.S., Cook, E.R., Barichivich, J., Christie, D.A., Villalba, R., LeQuesne, C., et al., 2020. Six hundred years of South American tree rings reveal an increase in severe hydroclimatic events since mid-20th century. *Proc. Natl. Acad. Sci. USA* 117, 16816–16823. <https://doi.org/10.1073/pnas.2002411117>.
- Moya, J., Lara, A., 2011. Cronologías de ancho de anillos de queñoa (*Polylepis tarapacana*) para los últimos 500 años en el Altiplano de la región de Arica y Parinacota. *Chile Bosque* 32, 165–173.
- Oberhuber, W., 2007. Limited by growth processes. In: Wieser, G., Tausz, M. (Eds.), *Trees at Their Upper Limit. Tree Life Limitation at the Alpine Timberline; Plant Ecophysiology*, Volume 5. Springer, Berlin, Germany, pp. 131–143.
- Ortega-Rodríguez, D.R., Hevia, A., Sánchez-Salguero, R., Santini, L., Pereira de Carvalho, H.W., Roig, F.A., Tomazello-Filho, M., 2022. Exploring wood anatomy, density and chemistry profiles to understand the tree-ring formation in Amazonian tree species. *Dendrochronologia* 71 (2022), 125915.
- Orvis, K.H., Grissino-Mayer, H.D., 2002. Standardizing the reporting of abrasive papers used to surface tree-ring samples. *Tree-Ring Res.* 47–50.
- Pabón-Caicedo, J.D., Arias, P.A., Carril, A.F., Espinoza, J.C., Borrel, L.F., Goubanova, K., Lavado-Casimiro, W., Masiokas, M., Solman, S., Villalba, R., 2020. Observed and projected hydroclimate changes in the andes. *Front. Earth Sci.* 8, 61. <https://doi.org/10.3389/feart.2020.00061>.
- Politis, D.N., Romano, J.P., 1994. The stationary bootstrap. *J. Am. Stat. Assoc.* 89 (428), 1303–1313.
- Quintilhan, M.T., Santini, L., Ortega Rodríguez, D.R., Guillemot, J., Cesilio, G.H.M., Chambi-Legoas, R., Nouvellon, Y., Tomazello-Filho, M., 2021. Growth-ring boundaries of tropical tree species: aiding delimitation by long histological sections and wood density profiles. *Dendrochronologia* 69, 125878. <https://doi.org/10.1016/J.DENDRO.2021.125878>.
- Reimer, P.J., Brown, T.A., Reimer, R.W., 2004. Discussion: reporting and calibration of post-bomb 14C data. *Radiocarbon* 46 (3), 1299e1304.
- Requena-Rojas, E.J., Morales, M., Villalba, R., 2020. Dendroclimatic assessment of *Polylepis rodolfo-vasquezii*: a novel *Polylepis* species in the Peru highlands. *Dendrochronologia* (2020). <https://doi.org/10.1016/j.dendro.2020.125722>.
- Requena-Rojas, E.J., Amoroso, M.M., Tisce-Otarola, G., Crispin-Delacruz, D.B., 2021. Assessing dendrochronological potential of *Escallonia myrtilloides* in the high andes of Peru. *Tree-Ring Res.* Vol. 77 (2), 41–52. <https://doi.org/10.3959/TRR2019-8>.
- Rodríguez-Caton, M., Andreu-Hayles, L., Morales, M.S., Daux, V., Christie, D.A., Coopman, R.E., Alvarez, C., Palat Rao, M., Aliste, D., Flores, F., Villalba, R., 2021. Different climate sensitivity for radial growth, but uniform for tree-ring stable isotopes along an aridity gradient in *Polylepis tarapacana*, the world's highest elevation tree species. *Tree Physiol.* 00, 1–19.
- Roig, F., Fernandez, M., Garcia, E., Altamirano, S., Monge, S., 2001. Dendrochronological studies in the humid Puna environments of Bolivia. *Rev. Boliv. Ecol.* 3–13.
- Romoleroux, K., 1996. Rosaceae 79. In: Harling, G., Andersson, L. (Eds.), *Flora of Ecuador*, 56. University of Gothenburg/Riksmuseum/ Pontificia Universidad Católica del Ecuador, Göteborg/Stockholm/ Quito, pp. 1–159.
- Rossi, S., Deslauriers, A., Gricar, J., et al., 2008. Critical temperatures for xylogenesis in conifers of cold climates. *Glob. Ecol. Biogeogr.* 17, 696–707.
- Santos, G.M., Xu, X., 2017. Bag of tricks: a set of techniques and other resources to help 14C laboratory setup, sample processing, and beyond. *Radiocarbon* 59 (3), 785–801.
- Santos, G.M., Granato-Souza, D., Barbosa, A.C., Oelkers, R., Andreu-Hayles, L., 2020. Radiocarbon analysis confirms annual periodicity in *Cedrela odorata* tree rings from the equatorial Amazon. 1195 *Quat. Geochronol.* 58, 101079. <https://doi.org/10.1016/j.quageo.2020.101079>.
- Scheel, M.L.M., Rohrer, M., Huggel, C., Santos Villar, D., Silvestre, E., Huffman, G.J., 2011. Evaluation of TRMM Multi satellite Precipitation Analysis (TMPA) performance in the Central Andes region and its dependency on spatial and temporal resolution. *Hydrol. Earth Syst. Sci.* 15, 2649–2663. <https://doi.org/10.5194/hess-15-2649-2011>.
- Schulman, E., 1956. *Dendroclimatic Changes in Semiarid America*. University of Arizona Press, Tucson.
- Servat, G.P., Mendoza, W., Hurtado, N., Castañeda, R., Olarte E., M., Alcocer F., R., 2013. "Growth, Regeneration, and Phenology of *Polylepis pauti* Hieron. (Rosaceae) Trees in a Montane Forest Ecotone of the Apurímac River Valley." in *Monitoring Biodiversity: Lessons from a Trans-Andean Megaproject*, edited by Alonso, Alfonso, Dallmeier, Francisco, and Servat, Grace P., 33–40.
- Simpson, B.B., 1979. A revision of the genus *Polylepis* (Rosaceae: Sanguisorbeae). *Smithson. Contr. Bot.* 43.
- Soliz, C., Villalba, R., Argollo, J., Morales, M.S., Christie, D.A., Moya, J., Pacajes, J., 2009. Spatio-temporal variations in *Polylepis tarapacana* radial growth across the Bolivian Altiplano during the 20th century. *Palaeogeogr. Palaeoclimatol. Palaeoecol.* 281, 296–308. <https://doi.org/10.1016/j.palaeo.2008.07.025>.
- Stahle, D.W., 1999. Useful strategies for the development of tropical tree-ring chronologies. *IAWA J.* 20 (3), 249–253.
- Suarez, L., Renison, D., Marcora, P., Hensen, I., 2008. Age – size – habitat relationships for *Polylepis australis*: dealing with endangered forest ecosystems. *Biodiversiti Conserv* 17, 2617–2625. <https://doi.org/10.1007/s10531-008-9336-1>.
- Thibeault, J.M., Seth, A., Garcia, M., 2010. Changing climate in the Bolivian Altiplano: CMLP3 projections for temperature and precipitation extremes. *J. Geophys. Res.* 115, D08103.
- Urrutia, R., Vuille, M., 2009. Climate change projections for the tropical Andes using a regional climate model: temperature and precipitation simulations for the end of the 21st century. *J. Geophys. Res.* 114, D02108. <https://doi.org/10.1029/2008JD011021>.
- Vera, C., Silvestri, G., Liebmann, B., Gonzalez, P., 2006. Climate change scenarios for seasonal precipitation in South America from IPCC-AR4 models. *Geophys. Res. Lett.* 33, L13707. <https://doi.org/10.1029/2006GL025759>.
- Vuille, M., Keimig, F., 2004. Interannual variability of summertime convective cloudiness and precipitation in the central Andes derived from ISCCP-B3 data. *J. Clim.* 17, 3334–3348.

- Vuille, M., Francou, B., Wagnon, P., Juen, I., Kaser, G., Mark, B.G., Bradley, R.S., 2008. Climate change and tropical Andean glaciers: past, present and future. *Earth-Sci. Rev.* 89, 79–96.
- Wang, L., Payette, S., Bégin, Y., 2002. Relationships between anatomical and densitometric characteristics of black spruce and summer temperature at tree line in northern Quebec. *Can. J. Res.* 32, 477–486.
- Weddell, H.A., 1861. *Chloris Andina*. Vol. 2. Bertrand. Paris, France.
- Wigley, T.M.L., Briffa, K.R., Jones, P.D., 1984. On the average value of correlated time series with applications in dendroclimatology and hydrometeorology. *J. Clim. Appl. Meteor.* 23, 201–213. [https://doi.org/10.1175/15200450\(1984\)023<0201:OTAVOC>2.0.CO;2](https://doi.org/10.1175/15200450(1984)023<0201:OTAVOC>2.0.CO;2).
- Zang, C., Biondi, F., 2015. treeclim: An R package for the numerical calibration of proxy-climate relationships. *Ecography* 38 (4), 431–436. <https://doi.org/10.1111/ecog.01335>.
- Zutta, B.R., Rundel, P.W., 2017. Modeled shifts in *Polylepis* species ranges in the Andes from the last glacial maximum to the present. *Forests* 8, 1–16.